Sr^+ single-ion clock

P Dubé[1], A A Madej[1,2] and B Jian[1,2]

[1] National Research Council Canada, Ottawa, Ontario, Canada K1A 0R6
[2] Department of Physics and Astronomy, York University, Toronto, Ontario, Canada M3J 1P3

E-mail: pierre.dube@nrc-cnrc.gc.ca

Abstract. The evaluated uncertainty of the $^{88}Sr^+$ ion optical clock has decreased by several orders of magnitude during the last 15 years, currently reaching a level of 1.2×10^{-17}. In this paper, we review the methods developed to control very effectively the largest frequency shifts that once were the main sources of uncertainty for the $^{88}Sr^+$ single-ion clock. These shifts are the micromotion shifts, the electric quadrupole shift and the blackbody radiation shift. With further improvements to the evaluation of the systematic shifts, especially the blackbody radiation shift, it is expected that the total uncertainty of the single-ion clock transition frequency will reach the low 10^{-18} level in the near future.

1. Introduction

The progress in the control and evaluation of the frequency shifts in optical clocks has been very rapid during the last decade. The reduction of uncertainties has often times been more than incremental, resulting from an understanding of the underlying physics that has led to breakthroughs in the control of the shifts. A number of optical atomic clocks based on neutral atoms in optical lattices or single ions in rf traps now have total evaluated uncertainties reaching the 10^{-17} to the 10^{-18} level [1, and references therein]. As time passes, more optical clocks are being reported with improved control of the systematic shifts at these levels of uncertainty.

In this paper we present an overview of the methods used to control the main systematic shifts of the $^{88}Sr^+$ ion that have allowed a reduction by four orders of magnitude of the total evaluated frequency uncertainty in the last 15 years [2–4]. The key methods are the minimization of micromotion, the electric quadrupole shift cancellation by Zeeman averaging of the magnetic sublevel energies [3, 5], and a high-accuracy measurement of the differential scalar polarizability $\Delta\alpha_0$ of the clock transition [4]. The latter allows a further reduction of the total micromotion shifts by more than two orders of magnitude and is an essential parameter in the evaluation of the blackbody radiation shift. An overview of the uncertainty budget is given to illustrate the relative contributions of the main shifts and the potential for the $^{88}Sr^+$ ion to realize the unperturbed clock transition frequency with a total uncertainty in the low 10^{-18} level.

2. $^{88}Sr^+$ ion clock

The optical frequency reference is realized by first trapping and cooling a single ion of $^{88}Sr^+$ in an rf quadrupole trap. As shown in figure 1, cooling is performed on the $5s\,^2S_{1/2} - 5p\,^2P_{1/2}$ transition at 422 nm. A repumper laser at 1092 nm prevents decay from the $^2P_{1/2}$ state to the metastable $^2D_{3/2}$ state during the cooling pulse.

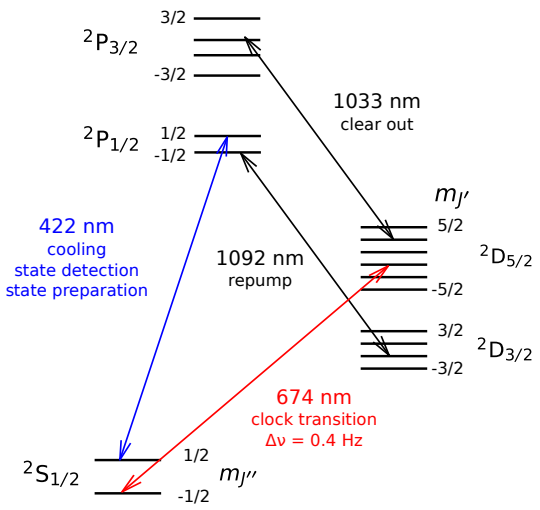

Figure 1. (color online) Partial energy level diagram of the $^{88}Sr^+$ ion.

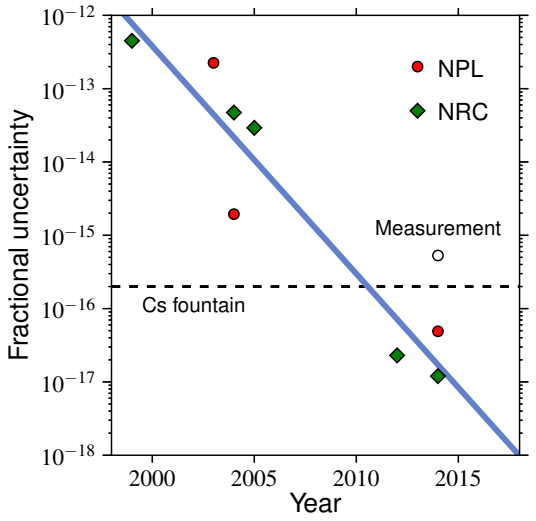

Figure 2. (color online) Evolution of the $^{88}Sr^+$ fractional frequency uncertainty.

The ion is typically cooled to temperatures of ≈ 2 mK in our setup [3, 6]. The reference frequency is realized by the 445 THz $5s\,^2S_{1/2}-4d\,^2D_{5/2}$ electric-quadrupole transition. It has a natural linewidth of 0.4 Hz determined by the 0.4 s lifetime of the $^2D_{5/2}$ state [7]. A small magnetic field of ≈ 1 μT is applied to the ion to split the S–D spectrum into ten resolved Zeeman components and define the quantization axis for optical pumping. There are no first-order magnetic insensitive resonances in the spectrum. Any of the five pairs of symmetric Zeeman components can be probed to obtain the virtual line center of the clock transition [8]. As described below, the experiments are performed by measuring and averaging the line centers of six Zeeman components to remove other frequency shifts.

The narrowest linewidth observed in our system is 4.4(3) Hz for 200 ms pulse lengths [3]. This was measured by recording scans that took ≈ 100 s to complete. For these long measurement times, the linewidth is partially broadened by laser and linear Zeeman shift frequency noise. When locking the laser to the clock transition, the update time for a single Zeeman component line center is comparatively much shorter, typically 8 s, which reduces the frequency noise contribution to the linewidth. In addition, the pulse duration is decreased to 100 ms to allow for a faster servo response. The resulting Fourier-transform-limited linewidth is ≈ 8 Hz.

A 1033 nm laser is used to transfer the ion from the metastable $^2D_{5/2}$ state to the short-lived $^2P_{3/2}$ state after the ion state has been determined from the 422 nm fluorescence levels. This action quickly returns the ion to the ground state in preparation for the final optical pumping step with circularly polarized 422 nm light. State-preparation ensures that the ion interacts with the probe laser light at each cycle. The stability obtained is $3\times10^{-15}/\sqrt{\tau}$ for 100 ms pulses [9].

Amplified spontaneous emission (ASE) light sources at 1033 nm and 1092 nm were developed recently as alternatives to their laser counterparts. In addition to providing a very compact package with no need for frequency stabilization and external shuttering, the 1092 nm broadband source has yielded lower ion kinetic temperatures than the laser source under the same experimental conditions [6].

3. Progress in evaluating the $^{88}Sr^+$ clock transition uncertainty

Figure 2 is a plot of the fractional frequency uncertainty of the $^{88}Sr^+$ ion as a function of year of publication [2–5, 10–14]. The first data point (year 1999) in figure 2 is the uncertainty of the

first and only Cs-based frequency synthesis chain measurement of $^{88}Sr^{+}$ [10]. The other data points report the evaluated uncertainty or the reproducibility of the clock transition frequency. As illustrated in figure 2, the uncertainty of the $^{88}Sr^{+}$ ion since 2012 has clearly surpassed that of Cs-based microwave standards. The most recent absolute frequency measurement of $^{88}Sr^{+}$ made with a cesium fountain clock (open circle in figure 2) is also shown for comparison [14].

4. Micromotion shifts

The micromotion shifts are caused by the interaction of the ion with the rf electric fields of the trap. The rf fields drive the ion motion at the trap frequency Ω, causing a second-order Doppler shift. They also cause scalar and tensor Stark shifts.

Micromotion shifts can be the most important sources of uncertainty in ion clocks when they are not properly minimized. For example, our first $^{88}Sr^{+}$ ion trap was not designed to control micromotion in three dimensions. As a consequence, its micromotion shifts are on the order of 30 Hz or $\approx 10^{-13}$ in fractional frequency units [4]. These large shifts were used for a high-accuracy measurement of the polarizability of the S–D transition as discussed in section 6. Micromotion caused by ion displacement is often called excess micromotion to distinguish it from the intrinsic micromotion caused by the thermal motion of the ion in the trapping potential [15, 16].

Our most recent trap of the endcap design [17] allows for proper minimization of excess micromotion. It has optical access ports for probing the ion motion along three mutually orthogonal directions and trim electrodes to adjust the ion position to the trap center. The micromotion-induced second-order Doppler and Stark shifts are reduced to the 10^{-17} level with minimization [2, 3]. Additional reduction is obtained by operating the trap at a special rf drive frequency as discussed in later sections.

5. Electric quadrupole shift

Unlike micromotion, the electric quadrupole shift (EQS) cannot be minimized with trim electrodes as it is an interaction between the $^2D_{5/2}$ state and an electric field gradient. The EQS is on the order of a few Hz in the endcap trap. It is the largest shift when micromotion is minimized.

The frequency shift Δf_Q of a magnetic sublevel $m_{J'}$ caused by the interaction between the quadrupole moment and an electric field gradient is given by [5, 18, 19]

$$\Delta f_Q = \frac{1}{4}\,\nu_Q\,\left(3\cos^2\theta - 1\right)\left[m_{J'}^2 - \frac{J'(J'+1)}{3}\right], \tag{1}$$

where ν_Q is a frequency proportional to the electric field gradient and the electric quadrupole moment [20]. θ is the angle between the electric field gradient principal axis and the quantization axis defined by the applied magnetic field [19]. $J' = 5/2$ refers to the upper $^2D_{5/2}$ state of the transition. The $^2S_{1/2}$ state has no quadrupole moment. Δf_Q describes the line center shift of symmetric Zeeman pairs since the two components of any pair have the same $m_{J'}^2$ value.

Two methods are commonly employed to cancel the EQS. One uses the property that the $\left(3\cos^2\theta - 1\right)$ term averages to zero when measurements are made for three mutually orthogonal magnetic field directions [19]. A limitation of this method is the requirement for a precise alignment of the magnetic field directions. On the other hand, it allows the use of a magnetic insensitive resonance to perform all the measurements.

The method we use is based on the observation that the term in square brackets in (1) vanishes when summing or averaging over the magnetic sublevels [3, 5, 21]:

$$\sum_{m_{J'}=-J'}^{J'}\left[m_{J'}^2 - \frac{J'(J'+1)}{3}\right] = 0. \tag{2}$$

This result is exact because the interaction Hamiltonian is traceless. Experimentally, (2) is realized by averaging the frequencies of six Zeeman components that connect to all of the $^2D_{5/2}$ state sublevels. The six components are grouped into three symmetric Zeeman pairs with $|m_{J'}| = 1/2,\ 3/2$ and $5/2$. Each Zeeman pair performs the function of canceling the linear Zeeman shift. Averaging the line centers of the three pairs of Zeeman components cancels the electric quadrupole shift according to (2).

The level of cancellation is extremely high, similar to that obtained for the linear Zeeman shift. We have attributed an uncertainty of 3×10^{-19} in canceling this shift, based on the possible bias that could occur due to changes in the magnetic field direction or in the strength of the electric field gradient during measurements. A revised uncertainty for the current setup would be lower since the evaluation was made before the ion stability was improved with state-preparation [3, 9]. In our experiments, the lock to the ion cycles through the six Zeeman components for a continuous evaluation and cancellation of the electric quadrupole shift. The tensor Stark shifts are also canceled by this method [3, 5].

6. Blackbody radiation shift

The interaction of the clock transition with the blackbody radiation (BBR) field, $\langle E^2 \rangle_T$, causes a Stark shift given by [22, 23]:

$$\Delta\nu_{\mathrm{BBR}} = -\frac{1}{2h}\langle E^2 \rangle_T \, \Delta\alpha_0 \, (1+\eta)\,, \tag{3}$$

where $\Delta\nu_{\mathrm{BBR}}$ is expressed in Hz. h is Planck's constant and $\Delta\alpha_0 = \alpha_0(^2D_{5/2}) - \alpha_0(^2S_{1/2})$ is the differential static scalar polarizability of the clock transition. η is a dynamic correction that accounts for the response of the atomic energy levels to the BBR spectrum.

The uncertainty evaluation of $\Delta\nu_{\mathrm{BBR}}$ depends on that of $\langle E^2 \rangle_T$, $\Delta\alpha_0$ and η. The values of $\Delta\alpha_0$ and η can be obtained from theoretical calculations or experimental measurements. The best theoretical calculations evaluate $\Delta\alpha_0$ with an uncertainty of 2×10^{-17} and η with an uncertainty of 8.4×10^{-20} [4, 24]. The current uncertainty estimate for $\langle E^2 \rangle_T$ in the endcap trap system is 1.1×10^{-17} [3].

Reduction of the $^{88}Sr^+$ uncertainty to the 10^{-18} level cannot be achieved without a more accurate determination of $\Delta\alpha_0$ and $\langle E^2 \rangle_T$. For the $^{88}Sr^+$ ion and other ions that have a positive scalar Stark shift, there is a convenient method for determining with high-accuracy the value of $\Delta\alpha_0$ [4]. The method is based on using large, applied micromotion shifts to compare the positive scalar Stark shift to the negative second-order Doppler shift. The trap drive frequency is then used to adjust the magnitude of the second-order Doppler shift for cancellation of the scalar Stark shift. This special trap drive angular frequency Ω_0 is directly related to $\Delta\alpha_0$ by the following relation [4]:

$$\Omega_0^2 \simeq -\frac{h\,\nu_0}{\Delta\alpha_0}\left(\frac{e}{mc}\right)^2, \tag{4}$$

where ν_0 is the clock transition frequency in Hz, e the elementary charge, m the mass of $^{88}Sr^+$ and c the speed of light.

Ω_0 was determined experimentally by comparing two trapped ions. One was in a test trap of Paul trap design with micromotion shifts at the 10^{-13} level. The other was in a reference endcap trap where the total shifts were at the 10^{-17} level. These trap systems were described in section 4. Note that the micromotion induced tensor Stark shift in the test trap was canceled by the Zeeman averaging method of section 5.

Figure 3 shows the experimental data of the trap comparison. The two ion clock transition frequencies agree when the test trap drive frequency is $\Omega_0/2\pi = 14.404(10)$ MHz. The reference trap was operated with a drive frequency of 14.39 MHz during these experiments. This

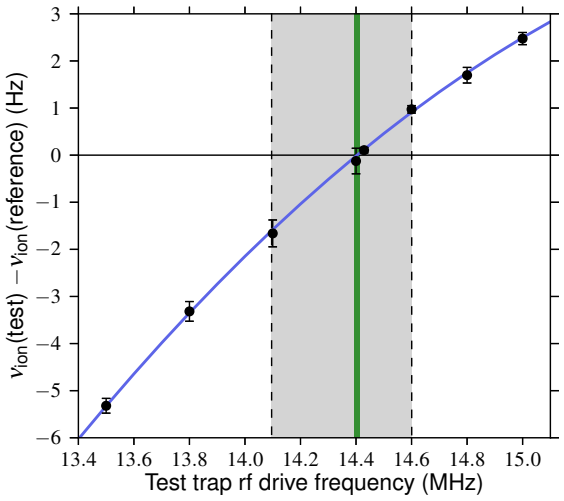

Figure 3. (color online) Comparison of the clock transition frequencies of two $^{88}Sr^+$ ions in different traps as a function of the rf drive frequency of the test trap [4]. The test trap has high micromotion shifts that vary with drive frequency. The narrow vertical band shows the value and uncertainty of the experimental determination of the drive frequency $\Omega_0/2\pi$ where the scalar Stark and second-order Doppler shifts cancel each other. The gray area is the predicted zone for the cancellation based on state-of-the-art theoretical calculations [24].

frequency was determined using (4) and a theoretical value of $\Delta\alpha_0$ [24]. From the experimental determination of Ω_0, we obtain $\Delta\alpha_0 = -4.7938(71) \times 10^{-40}$ J m^2/V^2 [4]. The reader is referred to previous work [4, 25] for a more accurate version of (4) that takes into account the second harmonic of ion motion. The BBR shift coefficient of the $^{88}Sr^+$ ion is calculated using (3) at 300 K, which gives $\Delta\nu_{\rm BBR}(300\ {\rm K}) = 0.247\,99(37)$ Hz. The fractional uncertainty of the frequency shift due to the uncertainty contributions of $\Delta\alpha_0$ has been reduced from 2×10^{-17} to 8.3×10^{-19} with this measurement. The evaluation of $\langle E^2 \rangle_T$ is now the most important source of uncertainty for our $^{88}Sr^+$ ion clock.

7. Uncertainty budget

Table 1 gives the current uncertainty budget for the $^{88}Sr^+$ ion in the reference endcap trap. It is a simplified and updated version of the budget given in [3]. The accurate measurement of $\Delta\alpha_0$ gives an improved evaluation of the BBR shift and a precise determination of the trap frequency for suppression of the micromotion shifts. By operating the endcap trap with a drive frequency of $\Omega_0 = 14.408(10)$ MHz, the net micromotion shifts are decreased from 10^{-17} to 10^{-19}. The test and endcap traps have slightly different values of Ω_0 because the ion motion direction and the Mathieu parameters are different in the two systems [25]. The total uncertainty is 1.2×10^{-17}, limited almost entirely by the BBR field evaluation. It is clear that a better evaluation of this field has the potential to reduce the total uncertainty of the $^{88}Sr^+$ ion to the low 10^{-18} level.

8. Conclusions

Several key methods were developed in recent years to deal very effectively with the most important sources of uncertainty in realizing the unperturbed frequency of the $5s\,^2S_{1/2} - 4d\,^2D_{5/2}$ clock transition of $^{88}Sr^+$. In addition to minimization of micromotion which is common to all ion optical clocks, Zeeman averaging is used to cancel the electric quadrupole shift and the tensor Stark shifts. We operate the ion trap with a special drive frequency Ω_0 that suppresses the net micromotion shifts by an additional factor of at least 200. The determination of $\Delta\alpha_0$ obtained from Ω_0 also provided an accurate value of the BBR shift coefficient, necessary for an accurate evaluation of the BBR shift. Further reduction of the total systematic shifts will require a better determination of the BBR field at the ion. The uncertainty budget indicates that a total uncertainty of $\approx 3 \times 10^{-18}$ should be attainable in the near future.

Table 1. Simplified uncertainty budget of the $^{88}Sr^{+}$ ion S–D frequency.

Source	mHz	Fractional
BBR field evaluation	4.9	1.1×10^{-17}
BBR coefficient ($\Delta\alpha_0$)	0.37	8.3×10^{-19}
Excess micromotion	0.05	1×10^{-19}
1092 nm ac Stark shift	1	2×10^{-18}
Second-order Doppler (thermal)	0.5	1×10^{-18}
Electric quadrupole shift	0.14	3×10^{-19}
Collisional shift	1	2×10^{-18}
Total uncertainty	5.1	1.2×10^{-17}

Acknowledgments
The authors gratefully acknowledge the important contributions of B. Hoger, W. Pakulski and R. Pelletier to the design and fabrication of several electronic components used in the single-ion clock system.

References
[1] Ludlow A D, Boyd M M, Ye J, Peik E and Schmidt P O 2015 *Rev. Mod. Phys.* **87** 637–701
[2] Madej A A, Dubé P, Zhou Z, Bernard J E and Gertsvolf M 2012 *Phys. Rev. Lett.* **109** 203002
[3] Dubé P, Madej A A, Zhou Z and Bernard J E 2013 *Phys. Rev.* A **87** 023806
[4] Dubé P, Madej A A, Tibbo M and Bernard J E 2014 *Phys. Rev. Lett.* **112** 173002
[5] Dubé P, Madej A A, Bernard J E, Marmet L, Boulanger J S and Cundy S 2005 *Phys. Rev. Lett.* **95** 033001
[6] Fordell T, Lindvall T, Dubé P, Madej A A, Wallin A E and Merimaa M 2015 *Opt. Lett.* **40** 1822–1825
[7] Letchumanan V, Wilson M A, Gill P and Sinclair A G 2005 *Phys. Rev.* A **72** 012509
[8] Bernard J E, Marmet L and Madej A A 1998 *Opt. Commun.* **150** 170–174
[9] Dubé P, Madej A A, Shiner A and Jian B 2015 *Phys. Rev.* A **92** 042119
[10] Bernard J E, Madej A A, Marmet L, Whitford B G, Siemsen K J and Cundy S 1999 *Phys. Rev. Lett.* **82** 3228–3231
[11] Margolis H S, Huang G, Barwood G P, Lea S N, Klein H A, Rowley W R C, Gill P and Windeler R S 2003 *Phys. Rev.* A **67** 032501
[12] Madej A A, Bernard J E, Dubé P, Marmet L and Windeler R S 2004 *Phys. Rev.* A **70** 012507
[13] Margolis H S, Barwood G P, Huang G, Klein H A, Lea S N, Szymaniec K and Gill P 2004 *Science* **306** 1355–1358
[14] Barwood G P, Huang G, Klein H A, Johnson L A M, King S A, Margolis H S, Szymaniec K and Gill P 2014 *Phys. Rev.* A **89** 050501
[15] Berkeland D J, Miller J D, Bergquist J C, Itano W M and Wineland D J 1998 *J. Appl. Phys.* **83** 5025–5033
[16] Keller J, Partner H L, Burgermeister T and Mehlstäubler T E 2015 *J. Appl. Phys.* **118** 104501
[17] Schrama C A, Peik E, Smith W W and Walther H 1993 *Opt. Commun.* **101** 32–36
[18] Abragam A 1978 *The Principles of Nuclear Magnetism* International series of monographs on physics (New York: Oxford University Press)
[19] Itano W M 2000 *J. Res. Natl. Inst. Stand. Technol.* **105** 829–837
[20] Barwood G P, Margolis H S, Huang G, Gill P and Klein H A 2004 *Phys. Rev. Lett.* **93** 133001
[21] Dubé P, Madej A A, Bernard J E and Shiner A D 2006 *Proceedings of the IEEE International Frequency Control Symposium and Exposition* (New York: IEEE) pp 409–414
[22] Itano W M, Lewis L L and Wineland D J 1982 *Phys. Rev.* A **25** 1233–1235
[23] Porsev S G and Derevianko A 2006 *Phys. Rev.* A **74** 020502
[24] Jiang D, Arora B, Safronova M S and Clark C W 2009 *J. Phys. B: At. Mol. Opt. Phys.* **42** 154020
[25] Dubé P, Madej A A, Tibbo M and Bernard J E 2014 *Proceedings of the 28$^{\text{th}}$ European Frequency and Time Forum* (Neuchâtel, Switzerland: IEEE) pp 443–446